

Robust Oscillations and Edge Modes in Nonunitary Floquet Systems

Vikram Ravindranath and Xiao Chen

Department of Physics, Boston College, Chestnut Hill, MA 02467, USA

(Dated: June 23, 2023)

We explore oscillatory behaviour in a family of periodically driven spin chains which are subject to a weak measurement followed by post-selection. We discover a transition to an oscillatory phase as the strength of the measurement is increased. By mapping these spin chains to free fermion models, we find that this transition is reflected in the opening of a gap in the imaginary direction. Interestingly, we find a robust, purely real, edge π -mode in the oscillatory phase. We establish a correspondence between the complex bulk spectrum and these edge modes. These oscillations are numerically found to be stable against interactions and disorder.

Introduction – Recent years have witnessed a growing interest in the monitored many-body quantum dynamics. It has been shown that there exists a generic entanglement phase transition in a unitary quantum dynamics subject to continuous monitoring [1–5]. By varying the monitoring strength, the individual quantum trajectory changes from a highly entangled volume-law phase to a disentangled area-law phase. Besides this phase transition, monitoring quantum dynamics can generate novel quantum phases, which exhibit quantum criticality or even host quantum orders [6–12]. Here the order can be conventional order or topological order, and is determined by the form of the measurement operator.

Most of these studies are focused on the static order in the steady state. In this paper, we explore quantum ordered phases with oscillatory behavior in a monitored qubit system. We investigate this behavior in a periodically driven non-unitary circuit. We show that the steady state can exhibit persistent oscillations between two ordered phases. Moreover, these oscillations break the discrete time-translation symmetry of the underlying dynamics, similar to time crystals which have been observed in disordered Floquet many-body localized systems [13–16]. In our model, the quantum order is protected by local “forced” measurements that prefer specific ordered configurations. Applied local unitaries flip between these ordered configurations, leading to oscillations.

In systems which can be mapped to models of free fermions, we demonstrate that such an oscillation behavior is due to a non-Hermitian analog of Majorana zero modes. Such an idea has been used to understand the ground state degeneracy in the Ising spin chain [17]. It has further been employed to understand “(almost) strong modes” that exhibit long coherence times in various static and driven Hermitian systems [18, 19]. In our model, the zero mode exists in an *imaginary* gap in the spectrum, is localized on the boundary and anti-commutes with the evolution operator, resulting in persistent oscillation behavior.

Non-unitary Floquet Dynamics – The dynamics of periodically-driven systems over one period T is governed by the *Floquet* operator \hat{V} [20]. Analogous to unitary

dynamics, in the non-unitary case, the dynamics of the quantum state is given by the repeated application of \hat{V} followed by an explicit normalization of the state,

$$|\psi(NT)\rangle = \frac{\hat{V}(NT)|\psi_0\rangle}{\|\hat{V}(NT)|\psi_0\rangle\|} = \frac{(\hat{V})^N|\psi_0\rangle}{\|(\hat{V})^N|\psi_0\rangle\|}, \quad (1)$$

where T has been set to 1. To understand the properties of the steady states – in the limit $N \rightarrow \infty$ – we need to analyze the spectrum of the \hat{V} operator.

It is also convenient to define an effective non-Hermitian Hamiltonian \hat{H}_F by expressing \hat{V} as $e^{-i\hat{H}_F}$. We denote the (complex) eigenvalues of \hat{H}_F by $\{E_n\}$, their corresponding right eigenstates by $\{|E_n\rangle\}$ and order them such that $\text{Im}\{E_j\} \geq \text{Im}\{E_{j+1}\}$. A generic initial state can be expressed as

$$|\psi_0\rangle = \sum c_j |E_j\rangle. \quad (2)$$

Under time evolution, the unnormalized state

$$|\psi(NT)\rangle = \sum_j c_j e^{-iE_j^R N} e^{E_j^I N} |E_j\rangle, \quad (3)$$

where $E_j^{R(I)}$ denotes the real (imaginary) part of E_j . Clearly, as $N \rightarrow \infty$, the quantum state approaches $|E_1\rangle$ with the largest E_1^I , provided that $c_1 \neq 0$.

In principle, a degeneracy in the imaginary direction can emerge so that $E_1^I = E_2^I = \dots = E_{N_S}^I$ for some $N_S \geq 2$. Generic initial states then do not evolve to a single final state; instead, they continue to evolve, even at late times, in the subspace spanned by $\{|E_1\rangle, |E_2\rangle, \dots, |E_{N_S}\rangle\}$. If the real parts E_j^R are uniformly separated so that $E_j^R \equiv E_0 + j \frac{2\pi}{N_S}$ the steady states can exhibit periodic behavior, with period N_S . In this paper, we focus on $N_S = 2$.

Free Fermions & “Zero” Modes – When the Hamiltonian \hat{H} can be mapped to a system of non-interacting fermions, the many-particle spectrum of \hat{H} can be built up by independently filling in the different single-particle energy levels. Since the many-particle energies are the sums of the energies of the occupied levels, a 2 dimensional steady state subspace manifests in the presence of

a single-particle mode c_0^\dagger , the imaginary part of whose eigenvalue ϵ_0 is 0. We term such modes that exist in the imaginary gap of the spectrum *i0 modes*, to distinguish them from the familiar zero modes that exist in a real gap. Many-body eigenstates can be grouped into pairs that differ solely in the occupation of c_0^\dagger . States in a pair have energies with the same imaginary part, and real parts offset by ϵ_0 .

With this picture in mind, given a \hat{V} which describes non-interacting fermions, the many-body spectrum of \hat{V} is now obtained from the product of its single-particle eigenvalues. A single-particle mode c_0^\dagger with the property that $\hat{V}c_0^\dagger = -c_0^\dagger\hat{V}$ ($= e^{-i\pi}c_0^\dagger\hat{V}$) generates a pairing of many-body states which differ in the occupation of c_0^\dagger , thereby having eigenvalues with the same absolute value, but differing in sign.

Model and setup – We consider a system of L spins subject to periodic, non-unitary driving, described by a Floquet operator \hat{V} . We study operators \hat{V} which can be written as a composition of an imaginary time evolution \hat{U}_I and a unitary operator \hat{U}_R . We also define the non-hermitian Floquet Hamiltonian \hat{H}_F . We consider a specific form for \hat{U}_I and \hat{U}_R , as shown below:

$$\begin{aligned} \hat{V} &= \hat{U}_I \hat{U}_R \\ \hat{U}_I &= e^{\beta \sum_j \hat{Z}_j \hat{Z}_{j+1}} \\ \hat{U}_R &= e^{-i \sum_j J_{zz,j} \hat{Z}_j \hat{Z}_{j+1}} e^{-i \sum_j J_{xx,j} \hat{X}_j \hat{X}_{j+1}} e^{-i h_y \sum_j Y_j} \\ \hat{H}_F &\equiv i \log \hat{V} \end{aligned} \quad (4)$$

\hat{X}_j, \hat{Y}_j and \hat{Z}_j refer to the Pauli operators acting non-trivially only on the spin at site j . The various parameters $\beta, J_{zz,j}, J_{xx,j}$ and h_j are all real. \hat{U}_I can be interpreted as a forced measurement with β being the strength of the measurement. \hat{U}_R is composed of unitaries that describe nearest-neighbor XX and ZZ couplings, and a pulse which rotates each spin by $2h_y$ about the Y -axis. The operator \hat{V} has a \mathbb{Z}_2 symmetry represented by the Parity operator $P = \prod_j \hat{Y}_j$, which represents a simultaneous π rotation of every spin about the Y -axis. The time evolution proceeds according to Eq. (1).

In the simplest case, where the pulses are near-perfect π -rotations about the Y -axis, the nearest-neighbor couplings $J_{xx} = J_{zz} = 0$, and the measurement strength $\beta \rightarrow \infty$, we expect to see oscillations between the two ordered phases $|\uparrow\uparrow\uparrow \dots\rangle$ and $|\downarrow\downarrow\downarrow \dots\rangle$. Our objective is to study the consequences of moving away from this fine tuned limit and examine if there exists a phase with finite β in which oscillations are present.

Bulk Spectrum – We begin by studying the single particle spectrum of the operator \hat{V} with a fixed β . The corresponding non-interacting Hamiltonian H_F has the form $\hat{H}_F = \frac{1}{4} \sum_{i,j} \gamma_i \mathcal{H}_{ij} \gamma_j$, with \mathcal{H} a complex, antisymmetric $2L \times 2L$ matrix and γ_i being majorana fermion

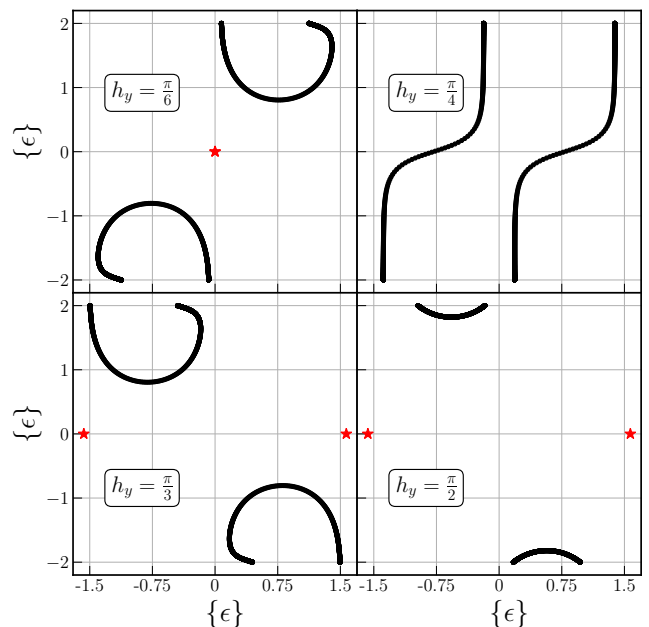


FIG. 1. Complex spectrum of \hat{H}_F given in Eq. (4) with $L = 1000$, $J_{xx} = 0.4$, $J_{zz} = 1$ and $\beta = 2$ with open boundary conditions for various h_y . The imaginary gap closes and reopens with the presence of a π -splitting between the $i0$ modes.

operators. This Hamiltonian can be diagonalized analogously to a Hermitian free fermion system [21], albeit now with a complex spectrum and complex majorana-like operators g_j .

$$\hat{H}_F = \frac{i}{2} \sum_{j=1}^L \epsilon_j g_{2j-1} g_{2j}. \quad (5)$$

Since the \hat{V} (hence also, \hat{H}_F) that we consider does not conserve particle number, we plot the quasi-energy spectrum in pairs of $\pm \frac{\epsilon}{2}$, where the $+$ ($-$) corresponds to a single particle state being occupied (unoccupied), resulting in $2L$ points being presented on each plot. A many-body eigenstate of \hat{V} is determined by choosing one mode in each of the L pairs. The process of obtaining and diagonalizing \hat{H}_F is detailed in [22].

We first focus on the regime where β is large. Consequently, the spectrum is gapped for a wide range of h_y . As h_y is varied, an eigenvalue gap closes and reopens in the imaginary direction. With open boundary conditions, $i0$ modes are present on either side of the gap closing. When h_y is small, the modes are degenerate. However, when h_y is tuned through the reopening of the imaginary gap, a π splitting between the real parts of the $i0$ modes emerges, as shown in Fig. 1. This is accompanied by the presence of oscillations in the steady state. The transition that we observe concerns the development of this robust splitting of π in the real values – not merely

the presence – of the $i0$ modes.

For the case where $J_{xx} = J_{zz} = 0$, the bulk spectrum of H_F , $\epsilon(k)$ can be obtained analytically.

$$\begin{aligned} \epsilon(k) &= \frac{i}{2} \log\left(z(k) \pm i\sqrt{1 - (z(k))^2}\right) \\ z(k) &= \cosh 2\beta \cos(2h_y) + i \sinh(2\beta) \sin(2h_y) \cos(k) \end{aligned} \quad (6)$$

The gap closing in the imaginary direction corresponds to $|z \pm i\sqrt{1 - z^2}| = 1$. This can only happen at $k = \frac{\pi}{2}$, requiring the condition

$$|\cosh(2\beta) \cos(2h_y)| > 1 \quad (7)$$

for the gap to remain open. The phases with and without a π -splitting between the real parts of the $i0$ modes' energies correspond to $\cosh(2\beta) \cos(2h_y) < -1$ and $\cosh(2\beta) \cos(2h_y) > 1$, respectively.

Edge $i0$ Modes – We now analyze the $i0$ modes and their real-space distribution in detail. We begin by delineating the role of an $i0$ mode. When the imaginary time evolution part of \hat{V} is sufficiently strong, the steady state is superposition of two states $\{|1\rangle, |2\rangle\}$ which have opposite parity and are the right eigenvectors of \hat{V} . These are degenerate, in the sense that $\hat{V}|i\rangle = \lambda_i|i\rangle$ for $i = 1, 2$, $|\lambda_1| = |\lambda_2|$ and $|\lambda_1| > |\lambda_j|$ for all other eigenstates $|j\rangle$ ($j \neq 1, 2$) of \hat{V} . An $i0$ mode is an operator \hat{F} that can toggle between $|1\rangle$ and $|2\rangle$.

Since it toggles between states of different parity, \hat{F} anticommutes with \hat{P} . Further, since $|\lambda_1| = |\lambda_2|$, $\hat{V}\hat{F} = e^{i\theta}\hat{F}\hat{V}$, with θ real. This can be seen from the effect of \hat{V} on a superposition of $|1\rangle, |2\rangle$, since if θ were complex, there would only be one steady state.

$$\begin{aligned} \hat{V}|\psi\rangle &= \hat{V}(a|1\rangle + b|2\rangle) = \hat{V}(a|1\rangle + b\hat{F}|1\rangle) \\ &= (a\hat{V}|1\rangle + e^{i\theta}b\hat{F}\hat{V}|1\rangle) = \lambda_1(a|1\rangle + e^{i\theta}b|2\rangle). \end{aligned} \quad (8)$$

Further, since this work considers models with a 2 dimensional steady-state space, we must have $\hat{F}^2|1\rangle = e^{2i\theta}|1\rangle$, and $\hat{F}^2|1\rangle = \hat{F}|2\rangle = |1\rangle$, implying $\theta = 0$ or π . In the case where $\theta = \pi$, oscillations with twice the period of the driving are observed, and \hat{V} and \hat{F} anticommute. There are two $i0$ modes $\hat{F}_{(L)}$ and $\hat{F}_{(R)}$, localized on the left and right boundaries, respectively. The localization of these $i0$ modes guarantees the double degeneracy of the steady states in the thermodynamic limit. For instance, in the limit where $\beta \rightarrow \infty$ and $h_y \approx \frac{\pi}{2}$, the steady states are $|n\rangle = \frac{1}{\sqrt{2}}(|\uparrow\uparrow\uparrow \dots\rangle + (-1)^n |\downarrow\downarrow\downarrow \dots\rangle)$ for $n = 1, 2$. The role of $\hat{F}_{(R)}$ is played by $\hat{Z}_{1(L)}$, and both $\hat{Z}_{1,L}$ anticommute with \hat{V} .

Summarizing, the $i0$ mode satisfies

1. $\{\hat{F}, \hat{P}\} = 0$
2. $\{\hat{F}, \hat{V}\} \rightarrow 0$ as $L \rightarrow \infty$
3. \hat{F} decays exponentially into the bulk

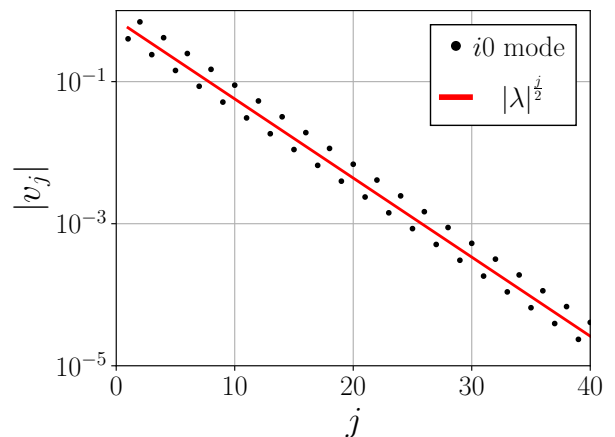


FIG. 2. A plot showing the exponential decay of the $i0$ mode for $L = 1000, h_y = \frac{\pi}{3}$ and $\beta = 2.0$, compared against the decay rate obtained analytically from Eq. (10).

$$4. \hat{F} = \sum_{j=1}^L v_{2j-1}a_j + v_{2j}b_j \text{ in free fermion systems}$$

Additionally, we require that $\hat{F}^2 \propto \mathbb{1}$, since the steady state space is 2 dimensional. This condition is trivially satisfied by the ansatz (4) for free fermion systems.

In the parameter regime shown in Fig. 1 with $h_y < \frac{\pi}{4}$, there are $i0$ modes as well, except with equal real parts. In this regime, although there are doubly degenerate steady states, oscillations are absent (i.e. $\theta = 0$). These $i0$ modes are obtained by replacing (2) with $[\hat{F}, \hat{V}] = 0$.

For \hat{F} , \vec{v} can be computed in the thermodynamic limit by using a transfer matrix method, which proceeds by rewriting the equation $\{\hat{F}, \hat{V}\} = 0$ as

$$\begin{pmatrix} v_{2j+2} \\ v_{2j+1} \end{pmatrix} = T \begin{pmatrix} v_{2j} \\ v_{2j-1} \end{pmatrix} \quad (9)$$

for $1 \leq j \leq L-2$. Crucially, this equation only holds for the bulk. We can choose to fulfill either the boundary equation which relates v_2 to v_1 (to obtain \hat{F}_L), or v_{2L} to v_{2L-1} (in the case of \hat{F}_R).

Here, we analytically solve for \vec{v} for $J_{xx} = J_{zz} = 0$. By imposing the boundary conditions for v_1 and v_2 , we find that

$$\begin{aligned} \begin{pmatrix} v_{2j} \\ v_{2j-1} \end{pmatrix} &= \lambda_1^{j-1} \begin{pmatrix} \cos(h_y) \\ \sin(h_y) \end{pmatrix} \\ \lambda_1 &\equiv i \cot(h_y) \coth(\beta) \end{aligned} \quad (10)$$

Requiring that this edge mode decays exponentially fast into the bulk, we have the condition

$$|\lambda_1| < 1 \implies \cosh(2\beta) \cos(2h_y) < -1, \quad (11)$$

which is *exactly* the condition for the band gap closing in the imaginary direction obtained in Eq. (7). Thus,

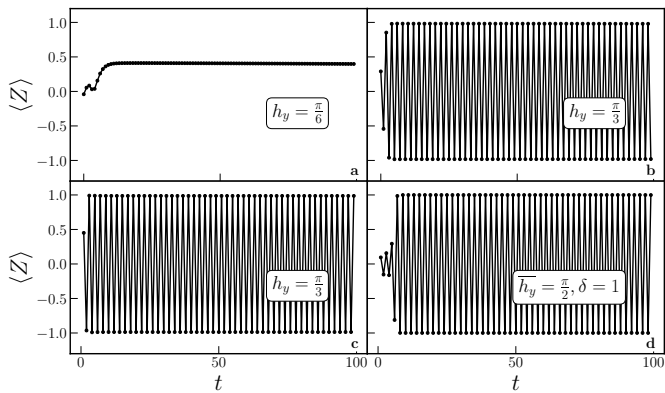


FIG. 3. Plots of $\langle Z \rangle$ without (a,b) and with interactions ((c,d), $J_{yy} = 0.3$). (a) Oscillations are absent and the $i0$ modes are degenerate. (b) Oscillations with double the period are present, and the $i0$ modes show a π splitting. (c) A clean interacting system. (d) A system with strong stochasticity in $h_{y,j}$. In all cases, $J_{xx} = 0.3, \beta = 0.75, L = 100$.

we have demonstrated a non-Hermitian bulk boundary correspondence. Extensions of Hermitian topological invariants have previously been used in studies that numerically obtained non-Hermitian edge modes [23, 24], adding to this correspondence.

We further compare this with the numerical results shown in Fig. 2. For $J_{xx}, J_{zz} \neq 0$, we can also numerically demonstrate that the $i0$ modes are localized on the edges.

Lastly, we introduce random spatial inhomogeneity in the Y -fields. h_y in Eq. (4) now assumes a position index j , i.e. $h_{y,j} = \frac{\pi}{3} \pm \delta \tilde{h}$, where \tilde{h} is uniformly drawn from $[-1, 1]$ for each site. Even in the presence of strong disorder, the $i0$ modes still persist [22], provided that the gap does not close in the imaginary direction.

The robustness of the edge modes requires $L \rightarrow \infty$ since the two edge modes can couple in small systems to produce a splitting in both the real and imaginary directions, resulting in a single steady state. The analysis of the splitting with finite L is presented in [22].

Dynamics and Interaction – We now turn to the dynamics to study the signature of these $i0$ modes. The dynamics can be simulated in two ways - first, by exploiting the mapping to free fermions and using the machinery of Fermionic Gaussian States (FGS)[25–30], and second, using MPS methods [31, 32] in terms of the spin degrees of freedom.

A limitation of FGS is that only Fermionic states with a definite parity can be simulated. Since \hat{V} conserves parity, the oscillations cannot be observed directly using FGS, since the two steady states $|\psi_{\pm}\rangle \sim |\uparrow\uparrow\uparrow \dots\rangle \pm i^L |\downarrow\downarrow\downarrow \dots\rangle$ have different parities. Instead, beginning with states of different parities, one can show that the final states at long times have an overlap ~ 1 with one of $|\psi_{\pm}\rangle$, providing indirect evidence for the presence of oscillations. A second limitation is that FGS cannot describe

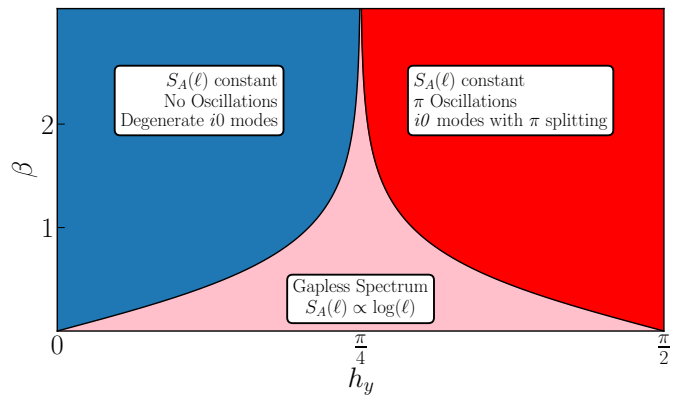


FIG. 4. A phase diagram summarizing the three different phases that are observed as β and h_y are tuned, in the case where $J_{yy} = J_{zz} = J_{xx} = 0$ and the phase boundary is analytically determined. The phase diagram remains qualitatively the same for nonzero J_{xx} and J_{zz} , with possibly more gap closings for larger J_{xx}, J_{zz} . The gapless critical phase is a special feature of non-unitary free fermion dynamics and will be replaced by a volume law phase in the presence of the interaction, e.g., $J_{yy} \neq 0$.

models with interactions. Thus, we use MPS methods to study the dynamics, utilizing the ITensor C++ Package [33].

We consider random product initial states $|\psi\rangle_0 = |\uparrow\uparrow\uparrow\downarrow\downarrow \dots\rangle$, where each spin points up or down along the z -axis. This state is stroboscopically evolved using Eq. (1), and the quantity $\langle Z(t) \rangle \equiv \frac{1}{L} \sum_j \langle \psi(t) | \hat{Z}_j | \psi(t) \rangle$ is calculated. Oscillations in $\langle Z \rangle$ occur when there are $i0$ modes with a difference of π in the real parts of their quasi-energies, and not otherwise (See Fig. 3).

Interactions are introduced including $e^{-iJ_{yy} \sum_j \hat{Y}_j \hat{Y}_{j+1}}$ in \hat{U}_R , which corresponds to a 4-fermion interaction $e^{-iJ_{yy} \sum_j \gamma_{2j-1} \gamma_{2j} \gamma_{2j+1} \gamma_{2j+2}}$. Such interactions can lead to thermalization in unitary models, which usually destabilizes any order [34, 35]. However, as shown in Fig. 3, oscillations persist in the presence of interactions.

Finally, we consider Y -fields that are random in both time and space, modeled as $e^{-i \sum_j h_{y,j}(t) \hat{Y}_j}$, where $h_{y,j}(t) = \bar{h}_y + \delta h_{y,j}(t)$, and $\tilde{h}_{y,j}(t)$ is drawn uniformly from $[-1, 1]$ at every time step. Again, oscillations persist, both in the interacting and the non-interacting models, confirming the stability of the $i0$ mode.

Discussion – In this work, we have studied the emergence of oscillatory behaviour in a periodically driven nonunitary system of qubits. We have found that a critical strength of measurement is required to observe oscillations that break the discrete time-translation symmetry in these systems. Such dynamical behavior is accompanied by the emergence of a non-Hermitian $i0$ mode, which is robust to various perturbations, both quenched

and stochastic. Such models can be realized in quantum circuits where 1- and 2-site unitary gates as in \hat{U}_R are applied to the qubits. The imaginary time evolution can be implemented by subjecting the system to weak measurements corresponding to the following Kraus operators at each site j

$$M_j^\pm = \frac{1}{\sqrt{2 \cosh(2\beta)}} \left(\cosh(\beta) \pm \sinh(\beta) \hat{Z}_j \hat{Z}_{j+1} \right) \quad (12)$$

and post-selecting for the $+$ outcome.

The steady states in either phase studied in the text obey an area law entanglement scaling. However, there is an intermediate regime between the two steady states where the spectrum is gapless in the imaginary direction. The transition from a regime where there is an imaginary gap in the spectrum of \hat{H}_F , to one where there isn't, is reflected in a change in the entanglement behavior of the steady states, from an area law to a (parameter-dependent) critical phase [6, 7, 36]. The properties of this phase are detailed in [22]. Fig. 4 shows the phase diagram for these non-interacting models as both h_y and β are varied.

Whereas we find oscillations even in clean systems, traditional time crystals rely on strong disorder to evade thermalization and thus exhibit order. In our models, the periodic weak measurements may be interpreted as effectively “cooling” the system to the steady-state subspace. The localization of the $i0$ mode on the edge and its spectral gap to bulk states lend additional explanations for this stability [17, 37], while unitary time crystals do not rely on such edge modes[13].

In future work, we hope to characterize the $i0$ mode in the presence of interactions. It is possible that such an operator might only pair states in a part of the spectrum of \hat{H}_F , but still provide detectable signatures in the dynamics. We would also like to study the role of symmetry breaking in these oscillations, and especially, how it might be used to generate oscillations of period greater than 2, and for the case of $N_S > 2$ steady states. Lastly, it would be interesting to understand if analogous $i0$ modes can be found in models that involve a rectification of the system based on measurement outcomes [38].

Acknowledgements. — We gratefully acknowledge computing resources from Research Services at Boston College and the assistance provided by Wei Qiu. This research is supported in part by the National Science Foundation under Grant No. DMR-2219735.

-
- [1] B. Skinner, J. Ruhman, and A. Nahum, Measurement-induced phase transitions in the dynamics of entanglement, *Physical Review X* **9**, 031009 (2019).
 [2] Y. Li, X. Chen, and M. P. A. Fisher, Quantum zeno effect

- and the many-body entanglement transition, *Phys. Rev. B* **98**, 205136 (2018).
 [3] A. Chan, R. M. Nandkishore, M. Pretko, and G. Smith, Unitary-projective entanglement dynamics, *Phys. Rev. B* **99**, 224307 (2019).
 [4] S. Choi, Y. Bao, X.-L. Qi, and E. Altman, Quantum error correction in scrambling dynamics and measurement-induced phase transition, *Physical Review Letters* **125**, 030505 (2020).
 [5] M. J. Gullans and D. A. Huse, Dynamical purification phase transition induced by quantum measurements, *Physical Review X* **10**, 041020 (2020).
 [6] X. Chen, Y. Li, M. P. A. Fisher, and A. Lucas, Emergent conformal symmetry in nonunitary random dynamics of free fermions, *Phys. Rev. Research* **2**, 033017 (2020).
 [7] O. Alberton, M. Buchhold, and S. Diehl, Entanglement transition in a monitored free-fermion chain: From extended criticality to area law, *Physical Review Letters* **126**, 10.1103/physrevlett.126.170602 (2021).
 [8] S. Sang and T. H. Hsieh, Measurement-protected quantum phases, *Physical Review Research* **3**, 10.1103/physrevresearch.3.023200 (2021).
 [9] A. Lavasani, Y. Alavirad, and M. Barkeshli, Measurement-induced topological entanglement transitions in symmetric random quantum circuits, *Nature Physics* **17**, 342 (2021).
 [10] M. Ippoliti, M. J. Gullans, S. Gopalakrishnan, D. A. Huse, and V. Khemani, Entanglement phase transitions in measurement-only dynamics, *Physical Review X* **11**, 10.1103/physrevx.11.011030 (2021).
 [11] S. Basu, D. P. Arovas, S. Gopalakrishnan, C. A. Hooley, and V. Oganesyan, Fisher zeros and persistent temporal oscillations in nonunitary quantum circuits, *Physical Review Research* **4**, 10.1103/physrevresearch.4.013018 (2022).
 [12] S.-K. Jian, Z.-C. Yang, Z. Bi, and X. Chen, Yang-lee edge singularity triggered entanglement transition, *Physical Review B* **104**, 10.1103/physrevb.104.1161107 (2021).
 [13] V. Khemani, A. Lazarides, R. Moessner, and S. L. Sondhi, Phase structure of driven quantum systems, *Phys. Rev. Lett.* **116**, 250401 (2016).
 [14] D. V. Else, B. Bauer, and C. Nayak, Floquet time crystals, *Phys. Rev. Lett.* **117**, 090402 (2016).
 [15] X. Mi, M. Ippoliti, C. Quintana, A. Greene, Z. Chen, J. Gross, F. Arute, K. Arya, J. Atalaya, R. Babbush, *et al.*, Time-crystalline eigenstate order on a quantum processor, *Nature* **601**, 531 (2022).
 [16] J. Randall, C. E. Bradley, F. V. van der Grienden, A. Galicia, M. H. Abobeih, M. Markham, D. J. Twitchen, F. Machado, N. Y. Yao, and T. H. Taminiau, Many-body-localized discrete time crystal with a programmable spin-based quantum simulator, *Science* **374**, 1474 (2021).
 [17] A. Y. Kitaev, Unpaired majorana fermions in quantum wires, *Physics-Uspekhi* **44**, 131 (2001).
 [18] J. Kemp, N. Y. Yao, C. R. Laumann, and P. Fendley, Long coherence times for edge spins, *Journal of Statistical Mechanics: Theory and Experiment* **2017**, 063105 (2017).
 [19] D. J. Yates, F. H. L. Essler, and A. Mitra, Almost strong $(0, \pi)$ edge modes in clean interacting one-dimensional floquet systems, *Phys. Rev. B* **99**, 205419 (2019).
 [20] L. Reichl, *The Transition to Chaos: Conservative Classical and Quantum Systems*, Vol. 200 (Springer Nature,

- 2021).
- [21] Y.-B. Guo, Y.-C. Yu, R.-Z. Huang, L.-P. Yang, R.-Z. Chi, H.-J. Liao, and T. Xiang, Entanglement entropy of non-hermitian free fermions, *Journal of Physics: Condensed Matter* **33**, 475502 (2021).
- [22] See Supplemental Material for details on the diagonalization of non-Hermitian free fermion systems, the transfer matrix method, the implementation of FGS, and the critical phase.
- [23] L. Zhou and J. Gong, Non-hermitian floquet topological phases with arbitrarily many real-quasienergy edge states, *Phys. Rev. B* **98**, 205417 (2018).
- [24] L. Zhou, Non-hermitian floquet topological superconductors with multiple majorana edge modes, *Phys. Rev. B* **101**, 014306 (2020).
- [25] S. Bravyi, Lagrangian representation for fermionic linear optics, *Quantum Info. Comput.* **5**, 216–238 (2005).
- [26] B. M. Terhal and D. P. DiVincenzo, Classical simulation of noninteracting-fermion quantum circuits, *Phys. Rev. A* **65**, 032325 (2002).
- [27] S. Bravyi and R. König, Classical simulation of dissipative fermionic linear optics, *Quantum Information & Computation* **12**, 925 (2012).
- [28] J. Surace and L. Tagliacozzo, Fermionic Gaussian states: an introduction to numerical approaches, *SciPost Phys. Lect. Notes* , 54 (2022).
- [29] X. Cao, A. Tilloy, and A. D. Luca, Entanglement in a fermion chain under continuous monitoring, *SciPost Phys.* **7**, 024 (2019).
- [30] X. Turkeshi, A. Biella, R. Fazio, M. Dalmonte, and M. Schiró, Measurement-induced entanglement transitions in the quantum ising chain: From infinite to zero clicks, *Phys. Rev. B* **103**, 224210 (2021).
- [31] S. Paeckel, T. Köhler, A. Swoboda, S. R. Manmana, U. Schollwöck, and C. Hubig, Time-evolution methods for matrix-product states, *Annals of Physics* **411**, 167998 (2019).
- [32] S. R. White and A. E. Feiguin, Real-time evolution using the density matrix renormalization group, *Phys. Rev. Lett.* **93**, 076401 (2004).
- [33] M. Fishman, S. R. White, and E. M. Stoudenmire, The ITensor Software Library for Tensor Network Calculations, *SciPost Phys. Codebases* , 4 (2022).
- [34] N. Regnault and R. Nandkishore, Floquet thermalization: Symmetries and random matrix ensembles, *Phys. Rev. B* **93**, 104203 (2016).
- [35] A. Lazarides, A. Das, and R. Moessner, Equilibrium states of generic quantum systems subject to periodic driving, *Phys. Rev. E* **90**, 012110 (2014).
- [36] C.-M. Jian, B. Bauer, A. Keselman, and A. W. Ludwig, Criticality and entanglement in non-unitary quantum circuits and tensor networks of non-interacting fermions, arXiv preprint arXiv:2012.04666 (2020).
- [37] J. K. Asbóth, L. Oroszlány, and A. Pályi, A short course on topological insulators, *Lecture notes in physics* **919**, 166 (2016).
- [38] M. McGinley, S. Roy, and S. A. Parameswaran, Absolutely stable spatiotemporal order in noisy quantum systems, *Phys. Rev. Lett.* **129**, 090404 (2022).
- [39] T.-C. Lu and T. Grover, Spacetime duality between localization transitions and measurement-induced transitions, *PRX Quantum* **2**, 040319 (2021).

Supplemental Material: Robust Oscillations and Edge Modes in Nonunitary Floquet Systems

Vikram Ravindranath and Xiao Chen
Department of Physics, Boston College, Chestnut Hill, MA 02467, USA

DIAGONALIZATION OF NON-HERMITIAN FREE FERMION HAMILTONIANS

Jordan-Wigner Transformation

The Jordan-Wigner transformation is a tool that is extensively used to map fermionic to spin- $\frac{1}{2}$ degrees of freedom. When $J_{yy} = 0$ in \hat{V} , this family of spin models maps to models of free fermions under the Jordan-Wigner transformation. The single-particle spectrum of these non-interacting models is easy to obtain numerically, even for very large system sizes. The full many-body spectrum is then built up by filling in the single particle eigenstates of \hat{V} . This transformation proceeds by identifying the spin operators with non-local fermionic operators. Nonlocality is required to accommodate the commutativity of spin operators on different sites. This transformation is defined using the prescription

$$\begin{aligned}\hat{Y}_j &\rightarrow i\gamma_{2j-1}\gamma_{2j} \\ \hat{X}_j &\rightarrow \left(\prod_{l<j} i\gamma_{2l-1}\gamma_{2l} \right) \gamma_{2j-1} \\ \hat{Z}_j &\rightarrow \left(\prod_{l<j} i\gamma_{2l-1}\gamma_{2l} \right) \gamma_{2j}\end{aligned}\tag{S1}$$

with $\{\gamma_j\}_{j=1}^{2L}$ being Majorana operators that obey $\{\gamma_k, \gamma_l\} = 2\delta_{kl}$. For ease of notation, we define $a_j = \gamma_{2j}$ and $b_j = \gamma_{2j-1}$, following [S1]. Under this transformation, the XX and ZZ couplings are expressed as

$$\hat{Z}_j\hat{Z}_{j+1} \rightarrow -ib_ja_{j+1}.\tag{S2}$$

By defining a column vector $\vec{\gamma}$ whose entries are the $2L$ majorana operators $\{\gamma_j\}$

$$\vec{\gamma} = \begin{pmatrix} b_1 \\ a_1 \\ \vdots \\ b_L \\ a_L \end{pmatrix},\tag{S3}$$

any noninteracting, fermionic, Hermitian Hamiltonian can be written in the form

$$H = \frac{\gamma^T \mathcal{H} \gamma}{4} = \frac{1}{4} \sum_{i,j} \gamma_i \mathcal{H}_{i,j} \gamma_j,\tag{S4}$$

where \mathcal{H} is a $2L \times 2L$ purely imaginary antisymmetric matrix. For instance, \mathcal{H}_{xx} is a tridiagonal matrix, composed of blocks of the Pauli matrix Y

$$\mathcal{H}_{xx} = \begin{pmatrix} 0 & & & & & \\ & 0 & i & & & \\ & -i & 0 & & & \\ & & & \ddots & & \\ & & & & 0 & i \\ & & & & -i & 0 \\ & & & & & & 0 \end{pmatrix}. \quad (\text{S5})$$

We relax the restriction that the entries of \mathcal{H} are purely imaginary when we consider non-Hermitian Hamiltonians.

Spectrum of Free Fermion Hamiltonians

Given a non-interacting (not necessarily Hermitian) Hamiltonian \hat{H} , we now discuss the steps involved in obtaining its spectrum. We start by reviewing this process in the case where \hat{H} is Hermitian.

The most general Hermitian, parity-conserving, quadratic, fermionic Hamiltonian can be written in terms of Majorana operators $\{\gamma_j\}$ as

$$H = \frac{\gamma_i \mathcal{H}_{ij} \gamma_j}{4}, \quad (\text{S6})$$

where \mathcal{H} can be written as i times a real, $2L \times 2L$ antisymmetric matrix \mathcal{G} , such that

$$\mathcal{H}^\dagger = (i\mathcal{G})^\dagger = -i\mathcal{G}^T = \mathcal{H}. \quad (\text{S7})$$

The spectrum of real even-dimensional antisymmetric matrices comes in pairs of $\pm i\lambda_j$; $\lambda_j \in \mathbb{R}$, with corresponding eigenvectors v_j, v_j^* , where the elements of v_j^* are the complex conjugates of those of v_j . \mathcal{G} then has the decomposition

$$X^T \mathcal{G} X = \begin{pmatrix} 0 & \lambda_1 & & & & \\ -\lambda_1 & 0 & & & & \\ & & 0 & \lambda_2 & & \\ & & -\lambda_2 & 0 & & \\ & & & & \ddots & \\ & & & & & 0 & \lambda_L \\ & & & & & -\lambda_L & 0 \end{pmatrix} \equiv \Sigma, \quad (\text{S8})$$

with X a real orthogonal matrix

$$X^T X = X X^T = \mathbb{1}; \quad X_{ij} \in \mathbb{R}. \quad (\text{S9})$$

The matrix X is constructed from the normalized eigenvectors of \mathcal{G} as

$$X = \frac{1}{\sqrt{2}} \begin{pmatrix} | & | & & | & | \\ v_1 + v_1^* & i(v_1 - v_1^*) & \cdots & v_L + v_L^* & i(v_L - v_L^*) \\ | & | & & | & | \end{pmatrix} \quad (\text{S10})$$

If we define a new set of majorana operators $\{g_j\}$

$$\vec{g} = X^T \vec{\gamma} \quad (\text{S11})$$

which also obey canonical anticommutation relations

$$\begin{aligned}
\{g_i, g_j\} &= \sum_{l,m} X_{im}^T X_{jl}^T \{\gamma_m, \gamma_l\} \\
&= 2 \sum_{l,m} X_{im}^T X_{jl}^T \delta_{lm} \\
&= 2(X^T X)_{ij} = 2\delta_{ij},
\end{aligned} \tag{S12}$$

this decomposition allows us to rewrite the Hamiltonian from Eq. (S6) as

$$H = \frac{1}{2} \sum_{j=1}^L i\lambda_j g_{2j-1} g_{2j}. \tag{S13}$$

Lastly, defining a set of complex fermionic operators $\{f_j, f_j^\dagger\}$

$$f_j = \frac{g_{2j} - i g_{2j-1}}{2}, \tag{S14}$$

we have diagonalized H

$$H = \sum_j \lambda_j \left(f_j^\dagger f_j - \frac{1}{2} \right). \tag{S15}$$

The many-body eigenstates of H can then be constructed by filling in the single particle states f_j^\dagger .

$$\begin{aligned}
|n_1, n_2, \dots, n_L\rangle &= \left(f_1^\dagger\right)^{n_1} \left(f_2^\dagger\right)^{n_2} \dots \left(f_L^\dagger\right)^{n_L} |0\rangle \\
H |n_1, n_2, \dots, n_L\rangle &= \left(E_0 + \sum_j \lambda_j n_j\right) |n_1, n_2, \dots, n_L\rangle
\end{aligned} \tag{S16}$$

Turning to non-Hermitian Hamiltonians, we no longer consider an \mathcal{H} which has purely imaginary entries. However, owing to the anticommutativity of $\{\gamma_j\}$, \mathcal{H} can still be expressed as an antisymmetric matrix. Further, one now has to distinguish between the right and left eigenvectors (both of H and \mathcal{H}), which are not simply related by Hermitian conjugation, as in the Hermitian case. Once these caveats are accounted for, diagonalization proceeds in analogous fashion. The following text expands and elaborates on the methods introduced in [S2].

The eigenvalues of a complex, antisymmetric matrix \mathcal{H} can still be written as pairs of $\pm\lambda_j$, with $\lambda_j \in \mathbb{C}$, now. Their corresponding (right) eigenvectors are no longer related by complex conjugation. Therefore, we update our notation as follows. We assume an unambiguous ordering of $\pm\lambda_j$ in the pair $(\lambda_j, -\lambda_j)$. This can be achieved, for instance, by choosing λ_j to have a positive real part, or a positive imaginary part, if $\lambda_j \in i\mathbb{R}$. We use this to label the right eigenvectors as

$$\begin{aligned}
\mathcal{H}v_{2j-1} &= \lambda_j v_{2j-1} \\
\mathcal{H}v_{2j} &= -\lambda_j v_{2j}
\end{aligned} \tag{S17}$$

The corresponding $2L \times 1$ dimensional left eigenvectors are labelled

$$\begin{aligned}
u_{2j-1} \mathcal{H} &= \lambda_j u_{2j-1} \\
u_{2j} \mathcal{H} &= -\lambda_j u_{2j}
\end{aligned} \tag{S18}$$

The eigenvectors of an antisymmetric matrix \mathcal{H} have the following properties :

1. If v is a right eigenvector with eigenvalue λ , v^T is a left eigenvector with eigenvalue $-\lambda$.

$$\mathcal{H}v = \lambda v \implies (\mathcal{H}v)^T = \lambda v^T \implies v^T \mathcal{H} = -\lambda v^T$$

2. With the ordering prescription described above, we have the following inner product rules

$$\begin{aligned} \text{i)} \quad & v_{2j-1}^T v_{2k} \propto \delta_{j,k} \\ \text{ii)} \quad & v_{2j}^T v_{2k-1} \propto \delta_{j,k} \\ \text{iii)} \quad & v_{2j-1}^T v_{2k-1} = 0 = v_{2j}^T v_{2k} \end{aligned}$$

$$\begin{aligned} \text{i)} \quad & v_{2j-1}^T \mathcal{H} v_{2k} = -\lambda_k v_{2j-1}^T v_{2k} = -\lambda_j v_{2j-1}^T v_{2k} \\ & \implies (\lambda_j - \lambda_k) v_{2j-1}^T v_{2k} = 0 \end{aligned}$$

$$\text{Case 1: } k \neq j \implies \lambda_j \neq \lambda_k \implies v_{2j-1}^T v_{2k} \propto \delta_{j,k}$$

$$\text{Case 2: } k \neq j \text{ but } \lambda_k = \lambda_j = \lambda$$

We have

$$\mathcal{H}(v_{2j}, v_{2k}) = -\lambda \tag{S19}$$

If $v_{2j-1}^T v_{2k} \neq 0$ and $v_{2j-1}^T v_{2j} \neq 0$, we can redefine

$$v_{2k} \rightarrow v_{2k} - \frac{v_{2j-1}^T v_{2k}}{v_{2j-1}^T v_{2j}} v_{2j} \implies v_{2j-1}^T v_{2k}.$$

Lastly, if $v_{2j-1}^T v_{2j} = 0$, but $v_{2j-1}^T v_{2k} \neq 0$, we can simply swap

$$v_{2k} \leftrightarrow v_{2j}, \text{ thus } v_{2j-1}^T v_{2k} \propto \delta_{j,k}$$

ii) follows from transposing i).

$$\begin{aligned} \text{iii)} \quad & v_{2j-1}^T \mathcal{H} v_{2k-1} = \lambda_k v_{2j-1}^T v_{2k-1} = -\lambda_j v_{2j-1}^T v_{2k-1} \\ & \implies (\lambda_j + \lambda_k) v_{2j-1}^T v_{2k-1} = 0 \implies v_{2j-1}^T v_{2k-1} = 0 \\ & v_{2j}^T \mathcal{H} v_{2k} = -\lambda_k v_{2j}^T v_{2k} = \lambda_j v_{2j}^T v_{2k} \\ & \implies (\lambda_j + \lambda_k) v_{2j}^T v_{2k} = 0 \implies v_{2j}^T v_{2k} = 0 \end{aligned} \tag{S20}$$

The assertion that $\lambda_j + \lambda_k \neq 0$ can be made because the eigenvalues and their corresponding eigenvectors have been ordered according to a particular rule that ensures that a pair of eigenvalues $\pm\lambda$ is always ordered in the same way, regardless of the position of their occurrence in the spectrum.

3. With the normalization that $v_{2j-1}^T v_{2j} = v_{2j}^T v_{2j-1} = 1$, the left eigenvectors corresponding to the eigenvalue pair $\pm\lambda_j$ are $(u_{2j-1}, u_{2j}) \equiv (v_{2j}^T, v_{2j-1}^T)$. Moreover, we have $u_j v_k = \delta_{j,k}$.

We are now ready to construct an analogous X for the general antisymmetric matrix, defined as

$$\begin{aligned} X &= \frac{1}{\sqrt{2}} \begin{pmatrix} | & | & & | & | \\ v_1 + v_2 & i(v_1 - v_2) & \cdots & v_{2L-1} + v_{2L} & i(v_{2L-1} - v_{2L}) \\ | & | & & | & | \end{pmatrix} \\ X^T X &= X X^T = \mathbb{1} \end{aligned} \tag{S21}$$

It can be straightforwardly verified that

$$X^T \mathcal{H} X = \begin{pmatrix} 0 & i\lambda_1 & & & \\ -i\lambda_1 & 0 & & & \\ & & 0 & i\lambda_2 & \\ & & -i\lambda_2 & 0 & \\ & & & & \ddots \\ & & & & & 0 & i\lambda_L \\ & & & & & -i\lambda_L & 0 \end{pmatrix} \equiv \Sigma, \tag{S22}$$

since

$$\mathcal{H}X = \frac{1}{\sqrt{2}} \begin{pmatrix} \lambda_1(v_1 - v_2) & i\lambda_1(v_1 + v_2) & \cdots & \lambda_L(v_{2L-1} - v_{2L}) & i\lambda_L(v_{2L-1} + v_{2L}) \end{pmatrix} \quad (\text{S23})$$

and

$$\begin{aligned} \frac{1}{2}(v_{2k-1} + v_{2k})^T(v_{2j-1} + v_{2j}) &= -\frac{1}{2}(v_{2k-1} - v_{2k})^T(v_{2j-1} - v_{2j}) = \delta_{k,j} \\ \frac{1}{2}(v_{2k-1} + v_{2k})^T(v_{2j-1} - v_{2j}) &= -\frac{1}{2}(v_{2k-1} - v_{2k})^T(v_{2j-1} + v_{2j}) = 0 \end{aligned} \quad (\text{S24})$$

We can similarly define a new set of majorana-like operators $\{g_j\}$ that obey canonical anticommutation relations

$$\vec{g} = X^T \vec{\gamma}. \quad (\text{S25})$$

and the Hamiltonian can be written as

$$H = \frac{1}{2} \sum_j i\lambda_j g_{2j-1} g_{2j} \quad (\text{S26})$$

However, $g_j^\dagger \neq g_j$, since X is a *complex* orthogonal matrix. This leads us to define 2 sets of complex fermionic operators $\{f_{L,j}, f_{L,j}^\dagger\}$ and $\{f_{R,j}, f_{R,j}^\dagger\}$, where $L(R)$ denote the left and right eigenstates of the operator H , respectively.

$$\begin{aligned} f_{R,j}^\dagger &= \frac{g_{2j} + ig_{2j-1}}{2} \\ f_{L,j} &= \frac{g_{2j} - ig_{2j-1}}{2} \end{aligned} \quad (\text{S27})$$

These operators have the following anticommutation relations

$$\begin{aligned} \{f_{R,j}^\dagger, f_{L,k}\} &= \delta_{j,k} \\ \{f_{R,j}^\dagger, f_{R,k}^\dagger\} &= 0 \\ \{f_{L,j}, f_{L,k}\} &= 0 \end{aligned} \quad (\text{S28})$$

Crucially, $(f_{R,j}^\dagger)^\dagger \neq f_{L,j}$. H can now be expressed in terms of these f operators as

$$\hat{H} = \sum_j \lambda_j \left(f_{R,j}^\dagger f_{L,j} - \frac{1}{2} \right). \quad (\text{S29})$$

The (right) vacuum state $|0\rangle_R$ of H is defined by

$$f_{L,j} |0\rangle_R = 0; \quad j = 1, 2, \dots, L \quad (\text{S30})$$

The right eigenstates are now constructed from the vacuum state of H , by the application of $f_{R,j}^\dagger$.

$$\begin{aligned} |n_1, n_2, \dots, n_L\rangle_R &= (f_{R,1}^\dagger)^{n_1} (f_{R,2}^\dagger)^{n_2} \cdots (f_{R,L}^\dagger)^{n_L} |0\rangle_R \\ H |n_1, n_2, \dots, n_L\rangle_R &= (E_0 + \sum_j \lambda_j n_j) |n_1, n_2, \dots, n_L\rangle_R \end{aligned} \quad (\text{S31})$$

We are interested in the right eigenstates of H since these will be used to construct the steady states of our non-unitary time evolution operator. An analogous process can be used to construct the left eigenstates of H .

For example, the steady state under the time evolution given by e^{-iH} is given by the eigenstate whose eigenvalue has the largest imaginary part.

$$|SS\rangle_R = \prod_{\text{Im}\{\lambda_j\} > 0} f_{R,j}^\dagger |0\rangle_R \quad (\text{S32})$$

Quasi-energy Spectrum of Non-interacting Floquet Operators

The penultimate step in calculating the spectrum of our non-interacting Floquet Hamiltonian $\hat{H}_F \equiv \frac{\gamma^T \mathcal{H}_F \gamma}{4}$ is to obtain \mathcal{H}_F from \hat{V} . This can be done by exploiting the Gaussian nature of the various operators in \hat{U}_R and \hat{U}_I . Generally, if one has

$$\hat{V} = e^{\frac{\tilde{\gamma}^T A_1 \tilde{\gamma}}{4}} e^{\frac{\tilde{\gamma}^T A_2 \tilde{\gamma}}{4}}$$

with $A_i^T = -A_i$, then

$$\begin{aligned} \hat{V} &= e^{\frac{\tilde{\gamma}^T A \tilde{\gamma}}{4}}; \\ e^A &\equiv e^{A_1} e^{A_2}. \end{aligned} \quad (\text{S33})$$

This can be shown by noting that

$$\left[\frac{\tilde{\gamma}^T A_1 \tilde{\gamma}}{4}, \frac{\tilde{\gamma}^T A_2 \tilde{\gamma}}{4} \right] = \tilde{\gamma}^T \frac{[A_1, A_2]}{4} \tilde{\gamma},$$

followed by an application of the BCH formula. If \hat{V} is now a Floquet operator, this property allows us to obtain the spectrum of A , which we have shown to be the single-particle spectrum of $\frac{1}{4} \gamma^T A \gamma$ (and thus, of \hat{V} as well).

When \hat{V} is invariant under translations, the spectrum can be obtained analytically. We show this for the case where $\hat{V} = e^{(\beta - iJ_{zz})H_{ZZ}} e^{-iJ_{xx}H_{XX}} e^{-ihH_Y}$. Explicitly, these Hamiltonians have the following expressions

$$\begin{aligned} H_{XX} &= i \sum_{j=1}^L a_j b_{j+1} \equiv \frac{\tilde{\gamma}^T \mathcal{H}_{XX} \tilde{\gamma}}{4} \\ H_{ZZ} &= -i \sum_{j=1}^L b_j a_{j+1} \equiv \frac{\tilde{\gamma}^T \mathcal{H}_{ZZ} \tilde{\gamma}}{4} \\ H_Y &= i \sum_{j=1}^L b_j a_j \equiv \frac{\tilde{\gamma}^T \mathcal{H}_Y \tilde{\gamma}}{4} \end{aligned} \quad (\text{S34})$$

with $(a_{L+1}, b_{L+1}) = \pm(a_1, b_1)$. The choice of (anti-) periodic boundary conditions only constrains the k values to be (half-) integer multiples of $\frac{2\pi}{L}$ and has no effect on the presence of a gap in the spectrum in the thermodynamic limit. We can now write \hat{V} in the form suggested by Eq. (S33).

$$\begin{aligned} \hat{V} &= e^{-i \frac{\tilde{\gamma}^T \mathcal{H}_F \tilde{\gamma}}{4}} \equiv e^{-i \hat{H}_F}, \\ \text{with } e^{-i \mathcal{H}_F} &= e^{(\beta - iJ_{zz}) \mathcal{H}_{ZZ}} e^{-iJ_{xx} \mathcal{H}_{XX}} e^{-ih \mathcal{H}_Y} \end{aligned} \quad (\text{S35})$$

Since each Hamiltonian decomposes into blocks for each k , we can write, denoting $\vec{\gamma}_k \equiv (a_k, b_k, a_{-k}, b_{-k})$,

$$\begin{aligned} \hat{H}_F &= \sum_{k>0} \frac{\vec{\gamma}_k^T \mathcal{H}_F(k) \vec{\gamma}_k}{4} \\ e^{-i \mathcal{H}_F(k)} &= e^{(\beta - iJ_{ZZ}) \mathcal{H}_{ZZ}(k)} \\ &\quad e^{-iJ_{XX} \mathcal{H}_{XX}(k)} e^{-ih \mathcal{H}_Y(k)} \end{aligned} \quad (\text{S36})$$

It is useful to note the k -space representation of the Hamiltonians

$$\begin{aligned}\mathcal{H}_{XX}(k) &= 2i \begin{pmatrix} 0 & \cos(k) & \sin(k) & 0 \\ -\cos(k) & 0 & 0 & -\sin(k) \\ -\sin(k) & 0 & 0 & \cos(k) \\ 0 & \sin(k) & -\cos(k) & 0 \end{pmatrix} \\ \mathcal{H}_{ZZ}(k) &= \mathcal{H}_{XX}(-k) \\ \mathcal{H}_Y(k) &= 2 \begin{pmatrix} \sigma_y & \\ & \sigma_y \end{pmatrix} = 2(\mathbb{1} \otimes \sigma_y)\end{aligned}\tag{S37}$$

The energy levels of the Hamiltonian \hat{H}_F correspond to $\frac{1}{2}$ times the eigenvalues of \mathcal{H}_F . This can be seen by considering each term in Eq. (S29), which can be rewritten as

$$\hat{H} = \sum_j \frac{\lambda_j}{2} \left(2f_{R,j}^\dagger f_{L,j} - 1 \right).\tag{S38}$$

Since the eigenvalues of $\left(2f_{R,j}^\dagger f_{L,j} - 1 \right)$ are ± 1 , this results in the contribution of each mode, and thus the single particle spectrum, being $\pm \frac{\lambda_j}{2}$.

In practice, we first find the eigenvalues of $e^{-i\mathcal{H}_F(k)}$ (analytically) or of , calculate their logarithms and then halve them to get the quasi-energy spectrum $\epsilon(k)$ of \hat{H}_F . Since \hat{V} is particle-hole symmetric, care must be taken to ensure the symmetry of the spectrum of \hat{H}_F about 0.

As a demonstration, we show how one calculates the spectrum for the case where $J_{XX} = J_{ZZ} = 0$. $\mathcal{H}_{ZZ}(k)$ has an interesting structure, in that it can be written as

$$\mathcal{H}_{ZZ}(k) = -2(\cos(k)\mathbb{1} \otimes \sigma_y + \sin(k)\tau_y \otimes \sigma_z)\tag{S39}$$

where $\tau_{x,y,z}$ and $\sigma_{x,y,z}$ denote the usual Pauli matrices acting in distinct spaces. Going forward, the \otimes will be omitted when its presence is obvious.

An immediate consequence of this structure is that $\left(\frac{\mathcal{H}_{ZZ}(k)}{2} \right)^2 = \mathbb{1}$, so that

$$\begin{aligned}e^{\beta\mathcal{H}_{ZZ}(k)} &= \cosh(2\beta)\mathbb{1} + \sinh(2\beta)\frac{\mathcal{H}_{ZZ}(k)}{2} \\ &= \cosh(2\beta) - \sinh(2\beta)(\cos(k)\sigma_y + \sin(k)\tau_y\sigma_z)\end{aligned}\tag{S40}$$

Similarly,

$$e^{-ih\mathcal{H}_Y(k)} = \cos(2h) - i\sin(2h)\sigma_y\tag{S41}$$

Multiplying the two matrices, and fixing $\tau_y = \pm 1$ (which leads to a degeneracy), $e^{-i\mathcal{H}_F(k)}$ is of the form $c_0(k) + \vec{c}(k)\vec{\sigma}$. The eigenvalues of $e^{-i\mathcal{H}_F(k)}$ can be obtained straightforwardly as $c_0 \pm \sqrt{\vec{c}\cdot\vec{c}}$. The single particle spectrum of $\hat{H}_F(k)$ is then

$$\epsilon(k) = \frac{i}{2} \log\left(c_0 \pm \sqrt{\vec{c}\cdot\vec{c}}\right)\tag{S42}$$

The numerical diagonalization of $e^{-i\mathcal{H}_F}$ possesses a caveat that is absent in the analytical procedure, owing to the Floquet nature of the problem. A logarithm of each eigenvalue of \mathcal{H}_F , followed by its halving, is required to obtain the single particle spectrum of \hat{H}_F . As a result, the numerical procedure cannot distinguish between the two $i0$ modes $\epsilon_{i0} = \pm \frac{\pi}{2}$, since these are both reflected as an $e^{\mp i\pi} = -1$ eigenvalue of $e^{-i\mathcal{H}_F}$. Should a point appear only at one of $\frac{\pi}{2}$, an additional verification that it is doubly degenerate is required, and this is indeed the case.

TRANSFER MATRIX METHOD TO OBTAIN EDGE MODES

In this section, we discuss the details of the transfer matrix method used to obtain the edge $i0$ modes. Concretely, we do this for $\hat{V} = e^{\beta\sum Z_j Z_{j+1}} e^{-i\sum hY_j}$. In terms of Majoranas, this corresponds to $\hat{V} = e^{-i\beta\sum_{j=1}^{L-1} b_j a_{j+1}} e^{h\sum_{j=1}^L b_j a_j}$. Requiring that $\{\hat{V}, a_j\} = \{\hat{V}, b_j\} = 0$ gives us the $2L$ equations

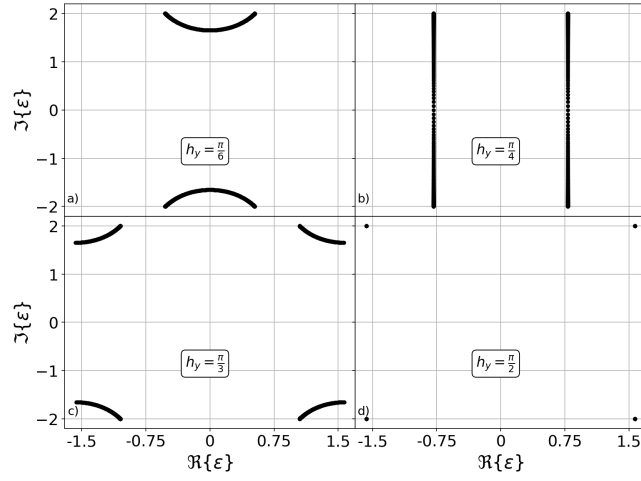


FIG. S1. The complex spectrum, showing a gap closing and reopening near $h_y = \frac{\pi}{4}$, as given by Eq. (7) in the main text.

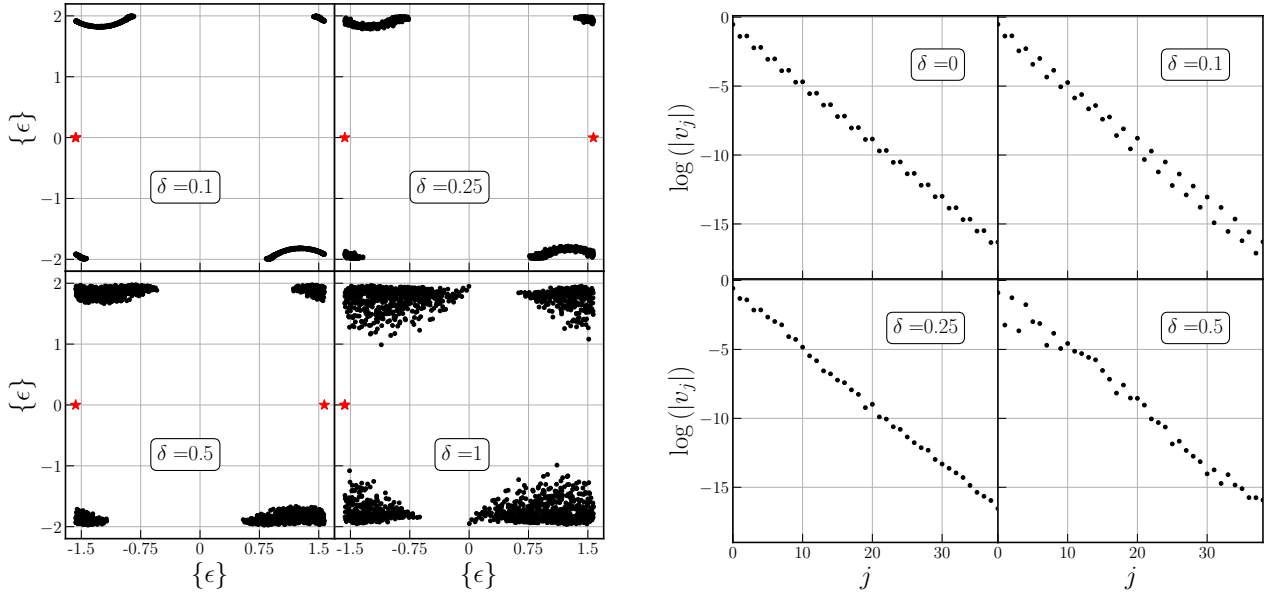


FIG. S2. (Left) Spectrum for the disordered case. (Right) Corresponding $i0$ mode \hat{F}_L . Open boundary conditions are considered.

$$a_1 : (\alpha_1 + 1)v_1 - \alpha_2 v_2 = 0 \quad (\text{S43})$$

$$\{b_j\}_{j=1}^{L-1} : \alpha_2 v_{2j-1} + (\alpha_1 + \alpha_3)v_{2j} + \alpha_4 v_{2j+1} = 0 \quad (\text{S44})$$

$$\{a_j\}_{j=2}^L : -\alpha_4 v_{2j-2} + (\alpha_1 + \alpha_3)v_{2j-1} - \alpha_2 v_{2j} = 0 \quad (\text{S45})$$

$$b_L : (\alpha_1 + 1)v_{2L} + \alpha_2 v_{2L-1} = 0 \quad (\text{S46})$$

with $\alpha_1 = \cos(2h)$, $\alpha_2 = \sin(2h)$, $\alpha_3 = \cosh(2\beta)$ and $\alpha_4 = i \sinh(2\beta)$, such that $\alpha_1^2 + \alpha_2^2 = \alpha_3^2 + \alpha_4^2 = 1$. Defining a matrix M as

$$M = \begin{pmatrix} \alpha_1 + 1 & -\alpha_2 & & & & & \\ \alpha_2 & \alpha_1 + \alpha_3 & \alpha_4 & & & & \\ & -\alpha_4 & \alpha_1 + \alpha_3 & -\alpha_2 & & & \\ & & \ddots & \ddots & \ddots & & \\ & & & & & \ddots & \\ & & & & & & \alpha_2 & \alpha_1 + 1 \end{pmatrix}, \quad (\text{S47})$$

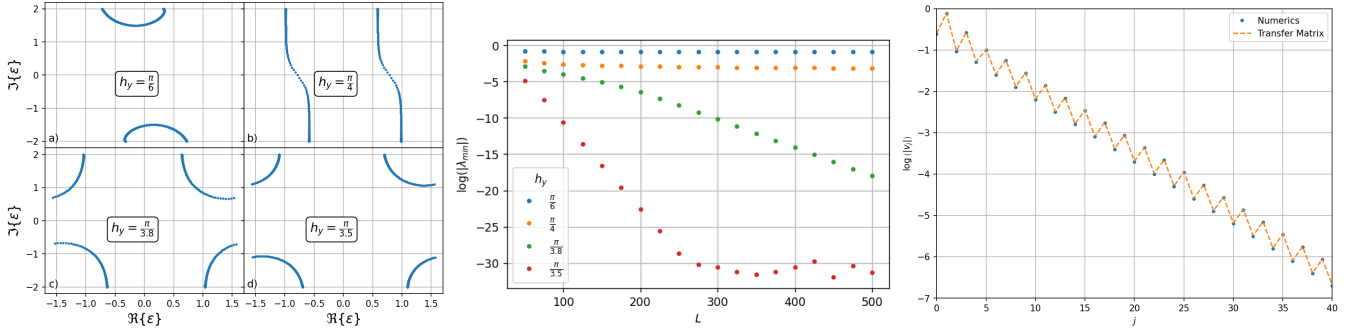


FIG. S3. (Left) The spectrum for different values of h_y , for $L = 1000$, $J_{xx} = 0.2$ and $\beta = 2$. (Center) The scaling of the magnitude of the smallest eigenvalue of T against L . When the system is in a non-trivial state, the smallest eigenvalue of M decays exponentially with L , but not otherwise. (Right) The decay of the $i0$ mode for $L = 1000$, $h_y = \frac{\pi}{3}$, $J_{xx} = 0.2$ and $\beta = 2.0$, compared against the eigenvector of M with the smallest magnitude eigenvalue

the problem now translates to finding the lowest magnitude eigenvectors \vec{v} of M , and to check whether their corresponding eigenvalues approach 0 exponentially as $L \rightarrow \infty$. We now explicitly construct \vec{v} using a transfer matrix approach.

Presently considering only the "bulk" equations, i.e. those pertaining to b_j, a_{j+1} for $1 \leq j \leq L - 1$, we can obtain $\begin{pmatrix} v_{2j+2} \\ v_{2j+1} \end{pmatrix}$ in terms of $\begin{pmatrix} v_{2j} \\ v_{2j-1} \end{pmatrix}$ as

$$\begin{pmatrix} v_{2j+2} \\ v_{2j+1} \end{pmatrix} = - \underbrace{\begin{pmatrix} \frac{(\alpha_1 + \alpha_3)^2 + \alpha_4^2}{\alpha_4 \alpha_2} & \frac{\alpha_1 + \alpha_3}{\alpha_4} \\ \frac{\alpha_1 + \alpha_3}{\alpha_4} & \frac{\alpha_2}{\alpha_4} \end{pmatrix}}_T \begin{pmatrix} v_{2j} \\ v_{2j-1} \end{pmatrix}. \quad (\text{S48})$$

Right away, we observe that $T = i\tilde{T}$, where \tilde{T} is a real, symmetric matrix. Further,

$$\det(T) = \frac{(\alpha_1 + \alpha_3)^2}{\alpha_4^2} + 1 - \frac{(\alpha_1 + \alpha_3)^2}{\alpha_4^2} = 1. \quad (\text{S49})$$

Thus, the eigenvalues of T are of the form $(i\lambda, \frac{-i}{\lambda}); \lambda \in \mathbb{R}$. Explicitly, the eigenvalues of T are $\lambda_{1,2} = i \frac{\cos(h) \cosh(\beta)}{\sin(h) \sinh(\beta)}, -i \frac{\sin(h) \sinh(\beta)}{\cos(h) \cosh(\beta)}$. Their corresponding eigenvectors are $\begin{pmatrix} \alpha_1 \pm 1 \\ \alpha_2 \end{pmatrix}$.

We now use the boundary equation for a_1 in order to fix the free parameters $\begin{pmatrix} v_2 \\ v_1 \end{pmatrix}$. Setting $\begin{pmatrix} v_2 \\ v_1 \end{pmatrix} = \begin{pmatrix} \cos(h) \\ \sin(h) \end{pmatrix} \propto \begin{pmatrix} \alpha_1 + 1 \\ \alpha_2 \end{pmatrix}$, we find that

$$\begin{pmatrix} v_{2j} \\ v_{2j-1} \end{pmatrix} = \lambda_1^{j-1} \begin{pmatrix} \cos(h) \\ \sin(h) \end{pmatrix}. \quad (\text{S50})$$

Lastly, we require that the edge mode localized around $j = 1$ decays exponentially, which imposes that

$$|\lambda_1| < 1 \implies \cosh(2\beta) \cos(2h) < -1, \quad (\text{S51})$$

We can analogously find the expression for the right edge mode by beginning with the boundary equation for b_L , and propagating leftwards with T^{-1} .

A few other checks were performed to confirm that the operator F obtained through the transfer matrix procedure is, in-fact, the $i0$ modes of interest. We first explicitly construct $\hat{F} = \sum_{j=1}^L v_{2j-1} a_j + v_{2j} b_j$, and represent it as a column vector

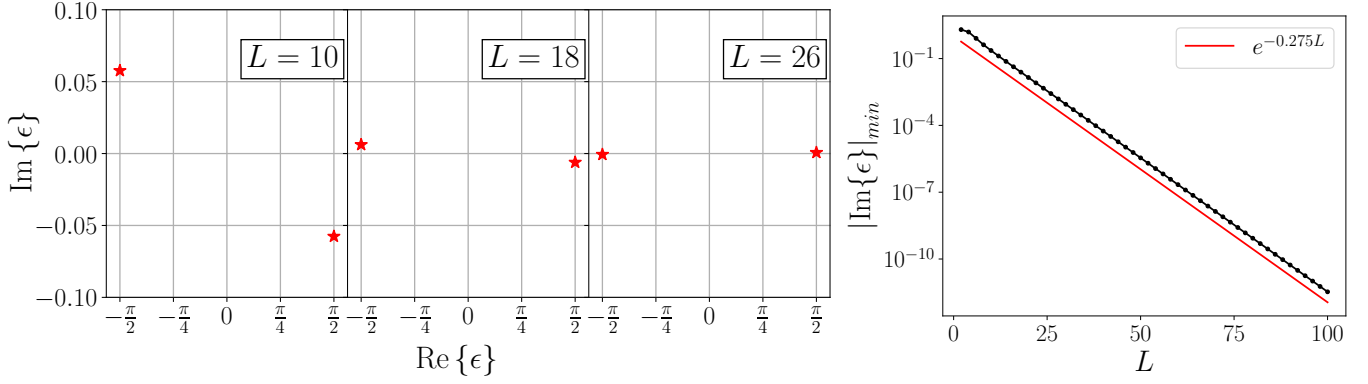


FIG. S4. Information about the single-particle spectrum of the model at $\beta = 2$, $h_y = \frac{\pi}{3}$ and $J_{xx} = J_{yy} = J_{zz} = 0$, for different system sizes L . (Left) A plot of the portion of the spectrum around $\text{Im}\{\epsilon\} = 0$, showing that there is a splitting in the imaginary direction induced by finite size effects. (Right) The splitting in the imaginary direction, defined as the minimum of the absolute values of imaginary parts of the eigenvalue, decays exponentially with system size L .

$$F_0 = \begin{pmatrix} v_2 \\ v_1 \\ v_4 \\ v_3 \\ \vdots \\ v_{2L} \\ v_{2L-1} \end{pmatrix}$$

so that it corresponds to the representation introduced in Eq. (S3). We find that $e^{-i\mathcal{H}_F} F_0 = -F_0$, confirming that $\{\hat{V}, \hat{F}\} = 0$.

While it might not be possible to analytically construct the edge modes for more general \hat{V} , it is straightforward to construct the matrix M and thus numerically obtain its smallest magnitude eigenvalue. Again, exponentially small eigenvalues appear exactly as we tune the parameters through a closing of the bulk gap in the imaginary direction. We show this below for $\hat{V} = e^{\beta \sum Z_j Z_{j+1}} e^{-i J_{xx} \sum X_j X_{j+1}} e^{-i \sum h Y_j}$.

Finally, we show in Fig. S3 that the $i0$ mode obtained by the direct diagonalization of \hat{V} is identical to the mode constructed from the transfer matrix, for nonzero J_{xx} .

TIME EVOLUTION OF FERMIONIC GAUSSIAN STATES

A fermionic many-body state $|\psi\rangle$ is said to be a Gaussian state [S3] if

$$|\psi\rangle\langle\psi| = \frac{e^{-\frac{\vec{v}_c^\dagger \mathcal{H}_G^c \vec{v}_c}{2}}}{\text{tr}\left(e^{-\frac{\vec{v}_c^\dagger \mathcal{H}_G^c \vec{v}_c}{2}}\right)} = \frac{e^{-\frac{\vec{\gamma}^\dagger \mathcal{H}_G \vec{\gamma}}{4}}}{\text{tr}\left(e^{-\frac{\vec{\gamma}^\dagger \mathcal{H}_G \vec{\gamma}}{4}}\right)} \quad (\text{S52})$$

for some $2L \times 2L$ matrix $\mathcal{H}_G^c = \mathcal{H}_G^{c\dagger}$ which has the form

$$\mathcal{H}_G^c = \begin{pmatrix} A_{L \times L} & B_{L \times L} \\ B_{L \times L}^\dagger & -A_{L \times L}^T \end{pmatrix} \quad (\text{S53})$$

with $A^\dagger = A$ and $B^T = -B$. For use in this section, we have defined \vec{v}_c analogously to $\vec{\gamma}$ as

$$\vec{v}_c = \begin{pmatrix} c_1 \\ c_2 \\ \vdots \\ c_L \\ c_1^\dagger \\ \vdots \\ c_L^\dagger \end{pmatrix}, \quad (\text{S54})$$

where $\{c_j, c_j^\dagger\}_{j=1}^L$ denote complex fermionic annihilation and creation operators at site j , obeying $\{c_j, c_k^\dagger\} = \delta_{j,k}$. These are related to $\{\gamma_j\}$ as

$$\begin{aligned} \gamma_{2j-1} &= i(c_j - c_j^\dagger) \\ \gamma_{2j} &= (c_j + c_j^\dagger) \end{aligned} \quad (\text{S55})$$

The relationship between $\vec{\gamma}$ and \vec{v}_c , and \mathcal{H}_G and \mathcal{H}_G^c can be succinctly expressed through the $2L \times 2L$ matrix W

$$W = \begin{pmatrix} i & 0 & \cdots & -i & 0 & \cdots \\ 1 & 0 & \cdots & 1 & 0 & \cdots \\ 0 & i & \cdots & 0 & -i & \cdots \\ 0 & 1 & \cdots & 0 & 1 & \cdots \\ & & & \vdots & & \\ 0 & \cdots & 1 & 0 & \cdots & 1 \end{pmatrix} \quad (\text{S56})$$

as

$$\vec{\gamma} = W\vec{v}_c \quad (\text{S57})$$

and

$$\mathcal{H}_G^c = \frac{1}{2}W^\dagger \mathcal{H}_G W. \quad (\text{S58})$$

$\frac{W}{\sqrt{2}}$ is a unitary matrix obeying $WW^\dagger = W^\dagger W = 2\mathbb{1}$, so \mathcal{H}_G^c and \mathcal{H}_G are unitarily similar and thus, share an eigenspectrum, as expected. For a quadratic fermionic Hamiltonian \hat{H} , this relation generally holds between the \mathcal{H} and \mathcal{H}^c , the matrices that represent \hat{H} in terms of majorana and complex fermions, respectively.

A Gaussian state obeys Wick's theorem, and every state that obeys Wick's Theorem can be expressed as in Eq. (S52). The expectation value in this state of any N -body operator can be written in terms of contractions involving the 2-point correlator $\langle \gamma_i \gamma_j \rangle$. Such states can be completely characterized in terms of their correlation matrices (or C -matrices)

$$\begin{aligned} C_{i,j}^m &= \langle \gamma_i \gamma_j \rangle \\ C_{i,j}^c &= \langle \vec{v}_{ci} \vec{v}_{cj}^\dagger \rangle \end{aligned} \quad (\text{S59})$$

where $c(m)$ denote the expectation values of complex (majorana) fermions. The two matrices are related as

$$C^m = WC^c W^\dagger \quad (\text{S60})$$

and

$$\begin{aligned} C^c &= (1 + e^{-\mathcal{H}_G^c})^{-1}, \\ C^m &= 2(1 + e^{-\mathcal{H}_G})^{-1}. \end{aligned} \quad (\text{S61})$$

The description of states that are defined on a 2^L dimensional Hilbert space has now been reduced to a description only involving $2L$ dimensions, avoiding the exponential growth of computational resources. Thus, instead of tracking the evolution of the state $|\psi\rangle$, it suffices to study its corresponding C - matrix, provided that the state under consideration always remains Gaussian.

Unitary Time Evolution of the C-Matrix

Under a time evolution governed by any fermionic Hamiltonian that is quadratic in the creation/annihilation operators, an initial Gaussian state always remains a Gaussian state. So, for some Hamiltonian $\hat{H} = \frac{\bar{v}_e^\dagger \mathcal{H}^c \bar{v}_e}{2}$, the time evolution of the C - Matrix is given as

$$\begin{aligned} C^c(t) &= \mathcal{U} C^c \mathcal{U}^\dagger \\ \mathcal{U}(t) &\equiv e^{-i\mathcal{H}t} \end{aligned} \quad (\text{S62})$$

Owing to the product rule Eq. (S33), the extension to Floquet systems proceeds using the Floquet Hamiltonian $\mathcal{U} = e^{-i\mathcal{H}_F^c}$ in Eq. (S62).

Non-Unitary Evolution - Establishing Gaussianity

It is not immediately obvious that \hat{V} maps one Gaussian state to another. In order to show this, we must make use of the product rule in Eq. (S33). Generalizing the evolution rule to density matrices, we have

$$\rho \rightarrow \frac{V\rho V^\dagger}{\text{tr}(V\rho V^\dagger)}, \quad (\text{S63})$$

where ρ is the density matrix $|\psi\rangle\langle\psi|$ corresponding to the pure state $|\psi\rangle$.

As with the time evolution of pure states, it is this explicit normalization that makes this time evolution non-linear. In the majorana representation, $\hat{V} = e^{-i\frac{\bar{\gamma}^\dagger \mathcal{H}_F \bar{\gamma}}{4}}$. Defining $\mathcal{V} = e^{-i\mathcal{H}_F}$, we have, by the product rule,

$$\begin{aligned} e^{-\frac{\bar{\gamma}^\dagger \mathcal{H}_G \bar{\gamma}}{4}} &\rightarrow e^{-\frac{\bar{\gamma}^\dagger \mathcal{H}'_G \bar{\gamma}}{4}} \\ e^{-\mathcal{H}'_G} &= \mathcal{V} e^{-\mathcal{H}_G} \mathcal{V}^\dagger \end{aligned} \quad (\text{S64})$$

Since \mathcal{H}_F and \mathcal{H}_G are antisymmetric, so is \mathcal{H}'_G . Further, the Hermiticity of \mathcal{H}_G ensures the Hermiticity of \mathcal{H}'_G . The resulting state $\rho' = \frac{e^{-\frac{\bar{\gamma}^\dagger \mathcal{H}'_G \bar{\gamma}}{4}}}{\text{tr}\left(e^{-\frac{\bar{\gamma}^\dagger \mathcal{H}'_G \bar{\gamma}}{4}}\right)}$ is also a Gaussian state. This proof relied only on the quadratic nature of \mathcal{H}_F and its antisymmetry, making it equally valid for unitary evolution. With the existence of a corresponding C' - matrix C' ensured, we now focus on relating C' to C .

Equations of Motion for C

The first method provides an equation of motion for the C - matrix, under the assumption that \hat{V} can be decomposed into a real time and imaginary time evolution. Unitary evolution is implemented directly by Eq. (S62). Then, using the fact that $C = (1 + e^{-\mathcal{H}_G^c})^{-1}$, defining an intermediate $\tilde{C}'(x) = (1 + e^{-x\mathcal{H}'_G} e^{-\mathcal{H}_G^c} e^{-x\mathcal{H}'_G})^{-1}$ and differentiating w.r.t x , we have

$$\frac{dC}{dx} = \{H_I, C\} + 2CH_I C \quad (\text{S65})$$

which can be numerically integrated to give the C - matrix.

Mapping Annihilation Operators

A more efficient approach is to directly construct the C - matrix at every time step. This process begins by noting that a pure state in this enlarged $2L$ dimensional space is *always* at “half-filling”, i.e. $\text{tr}(C) = L$. This means that for any state, there exist exactly L operators that annihilate it. For example, consider a 1-D chain which has the first N sites occupied

$$\begin{aligned} |\psi\rangle &= \prod_{j=1}^N c_j^\dagger |0\rangle, \\ c_j |\psi\rangle &= 0, j = N + 1 \cdots L, \\ c_j^\dagger |\psi\rangle &= 0, j = 1 \cdots N. \end{aligned} \quad (\text{S66})$$

Thus, $|\psi\rangle$ can be thought of as either N -filled sites, starting from the vacuum, or $L - N$ particles removed from the fully occupied chain. One finds that by simply keeping track of the operators that annihilate the state at a given time, the entire C - matrix can be recreated. In the basis of the operators that annihilate a state (represented as \vec{d}), with $d_j |\psi\rangle = 0; j = 1 \cdots L$, the only non-zero elements of the C - matrix are $\langle d_j d_j^\dagger \rangle = 1$. That is, in this basis,

$$C = \begin{pmatrix} \mathbb{1}_L & 0_L \\ 0_L & 0_L \end{pmatrix} \equiv C_0. \quad (\text{S67})$$

Secondly, for two bases $\{c_j, c_j^\dagger\}$ and $\{d_j, d_j^\dagger\}$ related by a unitary transformation $\vec{v}_c = \mathcal{U}\vec{v}_d$, the two C - matrices are related by

$$\begin{aligned} C &= \mathcal{U}C_0 \mathcal{U}^\dagger; \\ C_{ij} &= \sum_{l=1}^L \mathcal{U}_{i,l} \mathcal{U}_{l,j}^\dagger \end{aligned} \quad (\text{S68})$$

The transformation \mathcal{U} is guaranteed to be unitary since it is both linear and canonical (preserves commutation relations).

Finding \mathcal{U}

Consider an initial state $|\psi_0\rangle$ and a set of creation and annihilation operators $\{c_j, c_j^\dagger\}$ such that $c_j |\psi_0\rangle = 0, j = 1 \cdots L$. The evolution of this state is given by

$$\begin{aligned} |\psi_1\rangle &= \frac{\hat{V} |\psi_0\rangle}{\|\hat{V} |\psi_0\rangle\|}; \\ d_j |\psi_1\rangle &= 0, j = 1 \cdots L. \end{aligned} \quad (\text{S69})$$

We now wish to find \mathcal{U} that relates $\{c_j\}$ and $\{d_j\}$. Consider

$$\begin{aligned} \tilde{d}_j &\equiv \hat{V} c_j \hat{V}^{-1}; \\ \tilde{d}_j |\psi_1\rangle &\propto \hat{V} c_j \hat{V}^{-1} \hat{V} |\psi_0\rangle = 0. \end{aligned} \quad (\text{S70})$$

Right away,

$$\{\tilde{d}_j, \tilde{d}_l\} = \{\hat{V}c_j\hat{V}^{-1}, \hat{V}c_l\hat{V}^{-1}\} = \hat{V}\{c_j, c_l\}\hat{V}^{-1} = 0. \quad (\text{S71})$$

Since \hat{V} is Gaussian,

$$\tilde{d}_j = \sum_{l=1}^L \left(\mathcal{V}_{j,l}c_l + \mathcal{V}_{j,l+L}c_l^\dagger \right).$$

However, in general, $\{\tilde{d}_j^\dagger, \tilde{d}_l\} \neq \delta_{jl}$. This is resolved as follows.

We begin by writing each of the L annihilation operators as linear combinations of the canonical $\{c_j, c_j^\dagger\}$ operators. An arbitrary operator d_j can be written as

$$d_i = \vec{\alpha}_i^\dagger \vec{v}_c. \quad (\text{S72})$$

Instead of attempting to study operator evolution directly, we can instead focus on the $2L$ dimensional complex vector $\vec{\alpha}_i$. Under the evolution rule $c_j \rightarrow \hat{V}c_j\hat{V}^{-1} = \vec{\alpha}_i^\dagger \mathcal{V}^{-1} \vec{v}_c$, we can instead define the evolution as being generated by

$$\vec{\alpha}_i \rightarrow \vec{\beta}_i = (\mathcal{V}^{-1})^\dagger \vec{\alpha}_i. \quad (\text{S73})$$

Owing to the Gaussian nature of the time evolution, we can collect the L vectors corresponding to the L annihilation operators $\{c_j\}_{j=1}^L$ in a $2L \times L$ matrix, which we shall call \mathcal{U}_0 .

$$\mathcal{U}_0 \equiv \left(\begin{array}{c|c|c|c} | & | & \cdots & | \\ \vec{\alpha}_1 & \vec{\alpha}_2 & \cdots & \vec{\alpha}_L \\ | & | & & | \end{array} \right)_{2L \times L}. \quad (\text{S74})$$

By Eq. (S73), we have

$$\mathcal{U}_0 \rightarrow \tilde{\mathcal{U}}_1 = \left(\begin{array}{c|c|c|c} | & | & \cdots & | \\ \vec{\beta}_1 & \vec{\beta}_2 & \cdots & \vec{\beta}_L \\ | & | & & | \end{array} \right). \quad (\text{S75})$$

The operators given by $\tilde{d}_i \equiv \vec{\beta}_i^\dagger \vec{v}_c$ do not obey canonical commutation relations with their Hermitian conjugates. However, since $d_j |\psi_1\rangle = 0$, this is also true for any linear combination of the $\{d_j\}$. This implies that any vector constructed as a linear combination of $\{\vec{\beta}_i\}$ also describes an operator that annihilates $|\psi_0\rangle$. Additionally, since $\{\tilde{d}_j\}$ anticommute with each other, so too do their linear combinations. Therefore, we consider the vectors $\{\vec{\beta}_j\}$ obtained by orthonormalizing $\{\vec{\beta}_j\}$, collected in the matrix

$$\mathcal{U}_1 = \left(\begin{array}{c|c|c|c} | & | & \cdots & | \\ \vec{\beta}_1 & \vec{\beta}_2 & \cdots & \vec{\beta}_L \\ | & | & & | \end{array} \right). \quad (\text{S76})$$

The operators $\{d_j = \vec{\beta}_j^\dagger \vec{v}_c\}$ are canonical. We already showed in Eq. (S71) that they anticommute amongst themselves. Further,

$$\begin{aligned} \{d_i, d_j^\dagger\} &= \sum_{k,l=1}^L \left\{ (\beta_i)_k^* c_k + (\beta_i)_{k+L}^* c_k^\dagger, (\beta_j)_l c_l^\dagger + (\beta_j)_{l+L} c_l \right\} \\ &= \sum_{k,l=1}^L \left\{ (\beta_i)_k^* c_k, (\beta_j)_l c_l^\dagger \right\} + \left\{ (\beta_i)_{k+L}^* c_k^\dagger, (\beta_j)_{l+L} c_l \right\} \\ &= \sum_{k=1}^{2L} (\beta_i)_k^* (\beta_j)_k = \delta_{ij}. \quad [\text{By orthonormalization}] \end{aligned} \quad (\text{S77})$$

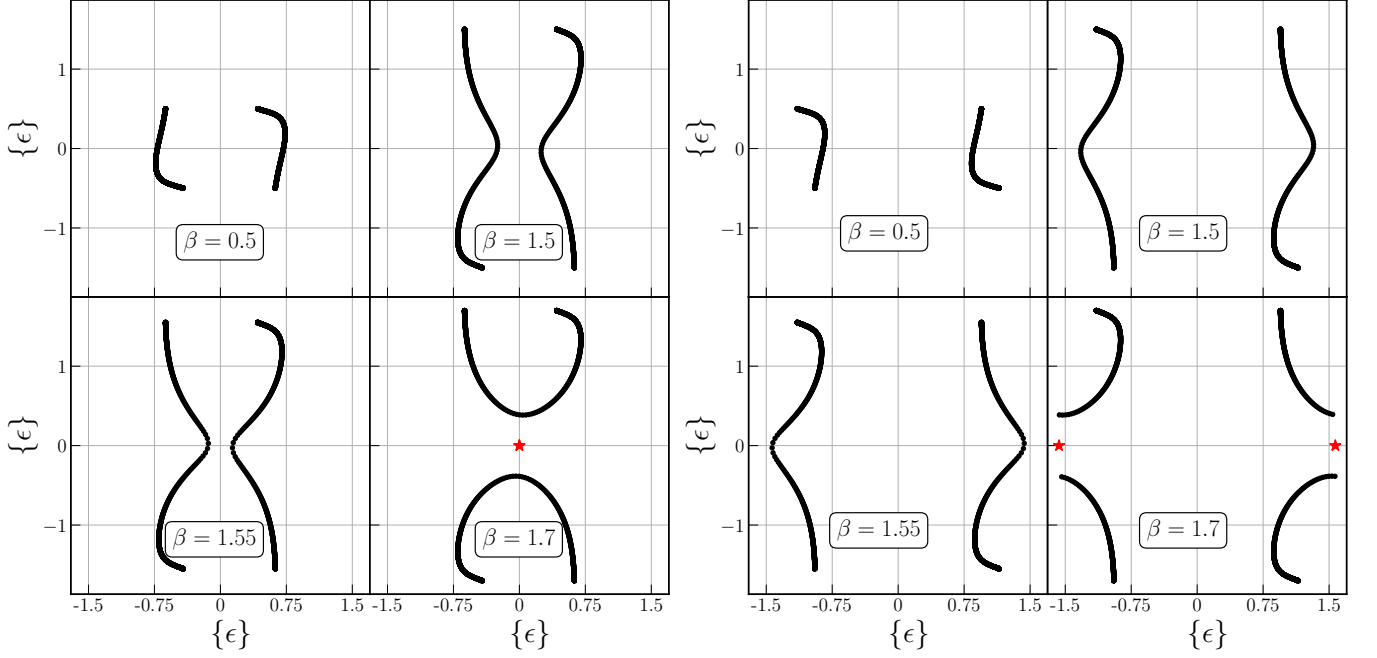


FIG. S5. Plots of the complex spectrum showing an imaginary gap opening as β is increased, revealing $i0$ modes (Left) with 0 splitting, $h_y = \frac{\pi}{6}$ (Right) with a π splitting, $h_y = \frac{\pi}{3}$ in the real direction.

The resulting $L \times 2L$ matrix \mathcal{U}_1^\dagger which relates $\{d_j\}_{j=1}^L$ to $\{c_j, c_j^\dagger\}$ is exactly the part of \mathcal{U}^\dagger that we require from Eq. (S68). Finally, we have

$$C = \mathcal{U}_1 \mathcal{U}_1^\dagger. \quad (\text{S78})$$

GAPLESS PHASE AND TRANSITIONS BY TUNING β

Lastly, we turn to the phase diagram as β is varied. When h_y is set to be appreciably close to $\frac{\pi}{2}$, we observe an imaginary gap open as β increases, leaving 2 $i0$ modes with a π splitting between their real parts. For h_y closer to zero, the $i0$ modes are degenerate instead.

As might be expected for these gapless modes, when the entanglement entropy of the steady state is considered, there is a transition from a critical, logarithmic to an area law scaling with the subsystem size. The coefficient of $\log(\sin(\frac{\pi L_A}{L}))$ in the critical phase is parameter dependent, in agreement with previous results on emergent conformal symmetry in non-unitary random free fermion models [S4–S6].

-
- [S1] T.-C. Lu and T. Grover, Spacetime duality between localization transitions and measurement-induced transitions, *PRX Quantum* **2**, 040319 (2021).
- [S2] Y.-B. Guo, Y.-C. Yu, R.-Z. Huang, L.-P. Yang, R.-Z. Chi, H.-J. Liao, and T. Xiang, Entanglement entropy of non-hermitian free fermions, *Journal of Physics: Condensed Matter* **33**, 475502 (2021).
- [S3] S. Bravyi, Lagrangian representation for fermionic linear optics, *Quantum Info. Comput.* **5**, 216–238 (2005).
- [S4] X. Chen, Y. Li, M. P. A. Fisher, and A. Lucas, Emergent conformal symmetry in nonunitary random dynamics of free fermions, *Phys. Rev. Research* **2**, 033017 (2020).
- [S5] O. Alberton, M. Buchhold, and S. Diehl, Entanglement transition in a monitored free-fermion chain: From extended criticality to area law, *Physical Review Letters* **126**, 10.1103/physrevlett.126.170602 (2021).
- [S6] C.-M. Jian, B. Bauer, A. Keselman, and A. W. Ludwig, Criticality and entanglement in non-unitary quantum circuits and tensor networks of non-interacting fermions, arXiv preprint arXiv:2012.04666 (2020).

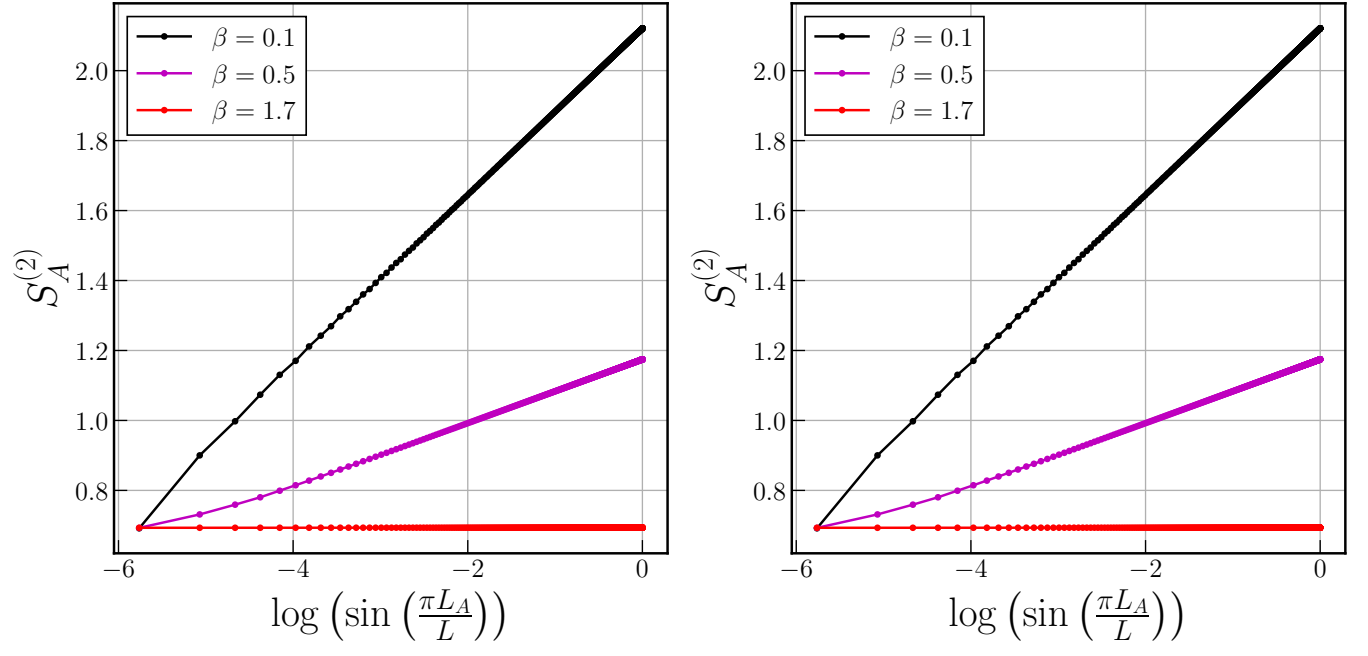


FIG. S6. Scaling of the entanglement entropy with subsystem size as β is increased. (Left) $h_y = \frac{\pi}{6}$ (Right) $h_y = \frac{\pi}{3}$. When the $i0$ modes are present, the entanglement entropy becomes independent of system size.